Classification and characterisation of magmatic-hydrothermal tourmaline by combining field observations and microanalytical techniques

IOP Conf. Series: Materials Science and Engineering **891** (2020) 012010 doi:10.1088/1757-899X/891/1/012010

Classification and characterisation of magmatic-hydrothermal tourmaline by combining field observations and microanalytical techniques

K Drivenes[1], W Brownscombe[2], R B Larsen[1], R Seltmann[2], J Spratt[2] and B E Sørensen[1]

[1] Norwegian University of Science and Technology, Department of Geoscience and Petroleum, 7491 Trondheim, Norway
[2] Natural History Museum, Cromwell Road, London SW7 5BD, Great Britain

E-mail: kristian.drivenes@ntnu.no

Abstract. Tourmaline from the St. Byron lobe of the Land's End granite, SW England, was assessed by macroscopic, optical and quantitative microanalytical methods. In total, seven types of tourmaline were distinguished. The seven types reflect different crystallisation environments and stages in the magmatic-hydrothermal transition. Types 1-3 are interpreted to represent a gradual transition from tourmaline crystallising from a silicate melt to precipitation from magmatic aqueous fluids. Types 5-7 crystallised at subsolidus conditions from a different fluid generation than types 1-3. These fluids may be magmatic or mixed with other fluids (e.g., meteoric or formation waters). The Sn-mineralisation in the area is mostly related to the latter fluid generation, and the mineralising potential is reflected by the tourmaline composition.

1. Introduction

Tourmaline is the most common borosilicate mineral in the crust . It is found in magmatic, metamorphic, and sedimentary rocks, but is perhaps best known for the striking, museum-grade crystals found in South America and Central Africa. It has the general formula $XY_3Z_6T_6O_{18}BO_3V_3W$, where the X-site is occupied by Na, K, Ca, Pb, and vacancies; the Y-site by Fe^{2+}, Mg, Mn, Li, Ti, Al, Fe^{3+}, and Zn; the Z-site by Al, Cr, Fe^{3+}, Mg, and Fe^{2+}; the T-site by Si, B, and Al; the B-site by B; the V-site by OH and O; and the W-site by OH, F, and O. Due to a crystal structure that can accommodate a large range of major, minor and trace elements, it has gotten a reputation for being a trash can mineral alongside other complex silicate minerals, such as amphiboles. In addition, tourmaline is strongly resistant to chemical and physical weathering, and is stable over an extended range of P-T-X conditions, hence, it is a good petrogenetic indicator [1] and has potential as a provenance mineral [2-4].

In granitic systems, tourmaline is predominantly found in S-type granites. Boron is generally incompatible in the early-forming granitic mineral assemblage and tourmaline forms late during magmatic differentiation, where it commonly succeeds biotite as the main ferromagnesian mineral. During the magmatic-hydrothermal transition, boron is preferentially partitioned into the aqueous phase ($D^{fluid/melt}$ = 1-3 [5-7]). Within the Cornubian Batholith of SW England, which has served as a field laboratory in this study, evidence of boron-rich fluids migrating through fracture systems in the crystallised granite and country rock can easily be observed as black, tourmaline-rich veins. There is a

well-established link between tourmaline veins and tin mineralisation [8]. However, the relationship is not exclusive, and boron is not recognised as a complexing element in the transportation of Sn in ore fluids [9]. A thorough classification and characterisation of tourmaline is important in order to track the magmatic-hydrothermal transition, indicate fluid sources, and distinguish potentially ore-bearing from barren systems. This can only be accomplished by including the full spectrum of analytical techniques; from field observations, through optical microscopy, to quantitative microanalytical studies. This study aims to classify the diversity of tourmaline found in the St Byron lobe of the Land's End granite in Cornwall, SW England, based on field relations, optical properties and mineral chemistry. It will serve as a foundation for future studies trying to interpret the chemical and physical fluctuations within the late stages of granite crystallization and the onset of a potentially ore-forming hydrothermal system; that is, the elusive magmatic-hydrothermal transition.

2. Analytical methods

Quantitative spot analyses of tourmaline were obtained by electron microprobe analysis (EPMA) and LA-ICP-MS at the Natural History Museum, London. Major and minor elements were analysed using a CAMECA SX100 microprobe at 20 kV and 20 nA. Na, Si, Al, and Mg were analysed on a TAP crystal; Mn and Fe on a LLIF; Ca, Ti, and Cl on a PET; K, Sr, and Sn on a LPET; and F on a LPC0 crystal.

Peak counting times varied between 10 (Na) and 30 (e.g., Mn and Sn) seconds, and detections limits typically varied between 170 (Mg) and 800 (F) µg/g. Trace elements, in addition to some major elements (^{7}Li, ^{23}Na, ^{24}Mg, ^{27}Al, ^{29}Si, ^{31}P, ^{43}Ca, ^{45}Sc, ^{49}Ti, ^{51}V, ^{52}Cr, ^{55}Mn, ^{59}Co, ^{60}Ni, ^{63}Cu, ^{66}Zn, ^{69}Ga, ^{72}Ge, ^{85}Rb, ^{88}Sr, ^{89}Y, ^{90}Zr, ^{111}Cd, ^{113}In, ^{118}Sn, ^{121}Sb, ^{133}Cs, ^{137}Ba, ^{139}La, ^{140}Ce, ^{141}Pr, ^{145}Nd, ^{147}Sm, ^{151}Eu, ^{157}Gd, ^{175}Lu, ^{181}Ta, ^{182}W, ^{208}Pb, ^{232}Th, and ^{238}U), were analysed by laser ablation inductively coupled plasma mass spectrometry (LA-ICP-MS) using a 193 nm ESI excimer laser coupled to a 7500cs Agilent ICP-MS. Spots of 45 µm were analysed for 60 seconds using a fluence of 3 Jcm^{-2} and a frequency of 10 Hz, each following 30 seconds of blank measurement. NIST 612 was used as a primary standard with BCR 2g and GSD as secondary standards. Tourmaline results were normalised to known Si values measured by EPMA in the same location prior to LA-ICP-MS. Structural formulae were calculated using WINCLASTOUR [10] normalising for T+Y+Z=15.

3. Classification of tourmaline

3.1. Macroscopic and field observations

In the Land's End granite, tourmaline occurs in a variety of structures and textures: As a trace or minor mineral disseminated in the granite matrix, in pegmatitic pockets, miarolitic cavities, quartz-tourmaline aggregations in the form of orbicules, sheets, and larger bodies +/- K-feldspar phenocrysts (massive quartz-tourmaline (-K-feldspar) rocks – MQT/MQTK), veins, and replacement of former granite. In the field, tourmaline is black, and genetic interpretation must be based on the textural and structural relationship with the granite. The obvious magmatic or hydrothermal textures can easily be distinguished (i.e., disseminations, pegmatites and veins), whereas the field relationship of other textures are ambiguous and their genetic models are controversial [11-14]. An overview of the samples, localities and analyses is listed in Table 1 and Fig. 1.

3.2. Optical microscopy

Optical microscopy reveals a multitude of generations and growth stages of tourmaline. Classification is conveniently based on colour in plane polarised light due to the commonly drastic changes and strong zoning patterns. Seven types are distinguished based on colour and the microtextures within the samples, where the first and final three may be grouped together as two main groups. Examples of the different tourmaline types are shown in Fig. 2.

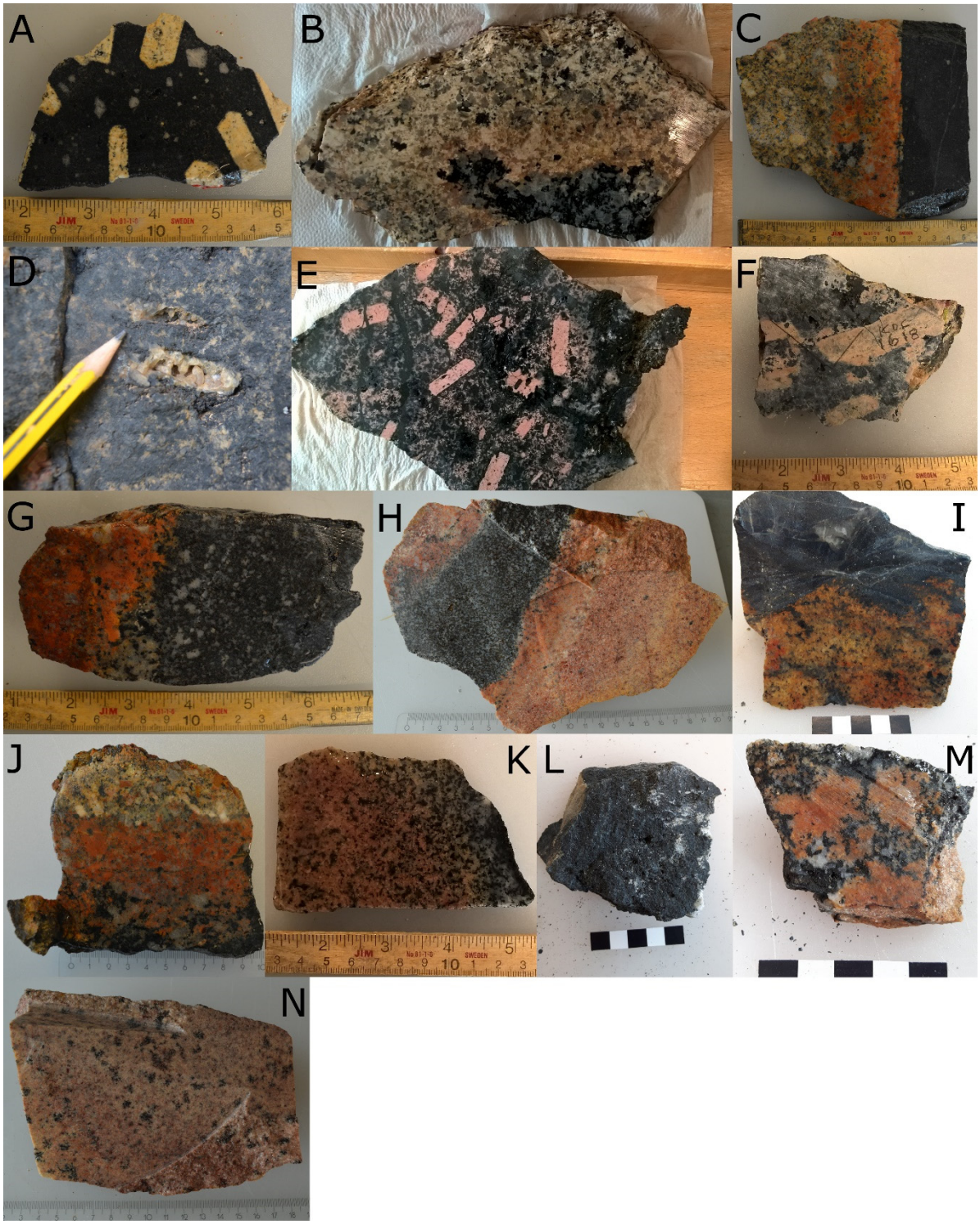

Figure 1. Samples investigated in this study. See Table 1 for a description and locality references. A: CAR-2. B: KDC-14-18. C: KDC-16-06. D: ES-102. E: KDC-14-14. F: KDC-16-18. G: KDC-16-08. H: KDC-16-12. I: KDC-17-02. J: KDC-16-05. K: KDC-16-19. L: KDC-17-03. M: KDC-17-08: N: KDC-16-13. Letters at the end of sample names in Table 1 refer to specific sections of the sample.

Table 1. Overview samples. See the text for a detailed description of the tourmaline types.

Sample	Lithology/texture	Locality	Tourmaline types	Short description
CAR-2	MQTK	Trevalgan	1,2,3,5	Fine-grained matrix of quartz and tourmaline (type 1,2,3) with K-feldspar phenocrysts. Euhedrally terminated type 3 tourmaline grow into small (few mm) miarolitic cavities. Minor alteration of K-feldspar phenocrysts by type 5 tourmaline.
ES-102	MQT	Nanjizal	1,2,3,5,6,7	Fine-medium grained matrix of quartz and clusters of type 5 tourmaline. Some large grains with multiple tourmaline generations were observed.
KDC-14-14-a	Replacement	Carn Barra	1,5	Fine-medium grained matrix of quartz and clusters of type 5 tourmaline. Minor type 1 tourmaline. Pink K-feldspar phenocrysts are cut by q-tur veins
KDC-14-18-c	Orbicule	Pellitras Point	1,6	Medium-coarse grained type 1 and 2 tourmaline and quartz. Minor type 6.
KDC-14-20-c	Replacement	Pellitras Point	1,2,3,4,5,6,7	Hydrothermal replacement of megacrystic coarse-grained granite. Local variations of tourmaline content. Mostly type 1 and 5
KDC-16-05-c	Q-tur sheet/vein	Carn Barges	1,4	Coarse-grained q-tur sheet. Mostly type 4 with minor type 1
KDC-16-06-aa	Q-tur sheet	Carn Barges	1,2,3,4	Fine-grained q-tur sheet cutting the coarse-grained megacrystic granite. Type 1, 2 and 3 in the sheet and minor type 4 in the contact to the granite.
KDC-16-08-b	Q-tur sheet	Carn Barges	1,2	Quartz-tourmaline sheet with equigranular matrix of type 1 and 2 tourmaline and quartz
KDC-16-12-c	Tur zone in tourmaline granite	Carn Barges	1,2,3,6	Quartz-tourmaline zone in a tourmaline granite. Mainly type 1 and 2, with minor type 3 and 6 tourmaline
KDC-16-13	Tourmline granite	Carn Barges	1	Interstitial type 1 tourmaline in the tourmaline granite matrix
KDC-16-18	Replacement	Pellitras Point	1,2,3,5,6,7	Hydrothermal replacement of megacrystic coarse-grained granite. Local variations of tourmaline content. Mostly type 1, 2 and 5
KDC-16-19-a	Q-tur zone in granite	Carn Barges	1,2,3	Quartz-tourmaline zone in a tourmaline granite with a central tourmaline zone. In the quartz-tourmaline zone, type 1 and 2 tourmaline is commonly overgrown by type 3. Type 3 becomes the dominant tourmaline type towards and in the tourmaline zone.
KDC-17-02-b	Altered FGG/tur zone	Pedn Vounder	1,2,3,5,6,7	Altered (K-metasomatism) fine-grained tourmaline granite with q-tur and tur zones. Great variation of tourmaline types
KDC-17-03	Miarole	Pedn Vounder	1,2,3,5,6	Tourmaline zone in the same rock as KDC-17-02. Highly variable tourmaline, but commonly type 1, 2 and 3, with overgrowths of type 6
KDC-17-08	Miarole	Carn Barges	1,2,3,4	Tourmaline growing in a miarolitic cavity in a fine-grained tourmaline granite. Mainly type 1,2 and 3, with minor type 4
KDC-17-12	MQT	Pedn Vounder	1,2,3	Fine-grained quartz and tourmaline (type 1,2,3) matrix with quartz phenocrysts.

Type 1 tourmaline is brown to orange, often weakly zoned from light to slightly darker brown. In sections normal to the c-axis, the core is commonly lighter in colour than the outer zones. This generation occasionally shows sector zoning. In disseminated tourmaline and orbicules, type 1 is the main, commonly the only, generation, with only minor occurrence of type 6. It is also represented as cores in tourmaline in quartz-tourmaline sheets and bodies (Figs. 2 k and 2 l), and less so in some replacement textures (Fig. 2h)

Type 2 tourmaline is weakly oscillatory zoned. This is observed as concentric, 10 - 200 μm, light brown and light blue bands around the c-axis. The thicker bands may be brown or blue depending on the sample. Type 2 typically occurs as the second growth stage following type 1, with or without resorption of type 1, and is commonly followed by type 3 tourmaline. This generation is common in quartz-tourmaline sheets and bodies (Figs. 2a, 2d, 2e, 2f, 2k and 2l).

Type 3 tourmaline is blue, and typically overgrows type 1 and 2 in tourmaline sheets and bodies. The contact between type 1 and 3 is commonly abrupt, whereas the contact between type 2 and 3 is more gradual. In some samples, type 3 is strongly oscillatory zoned. We found type 3 tourmaline in the same samples as type 2 (Figs. 2a and 2i).

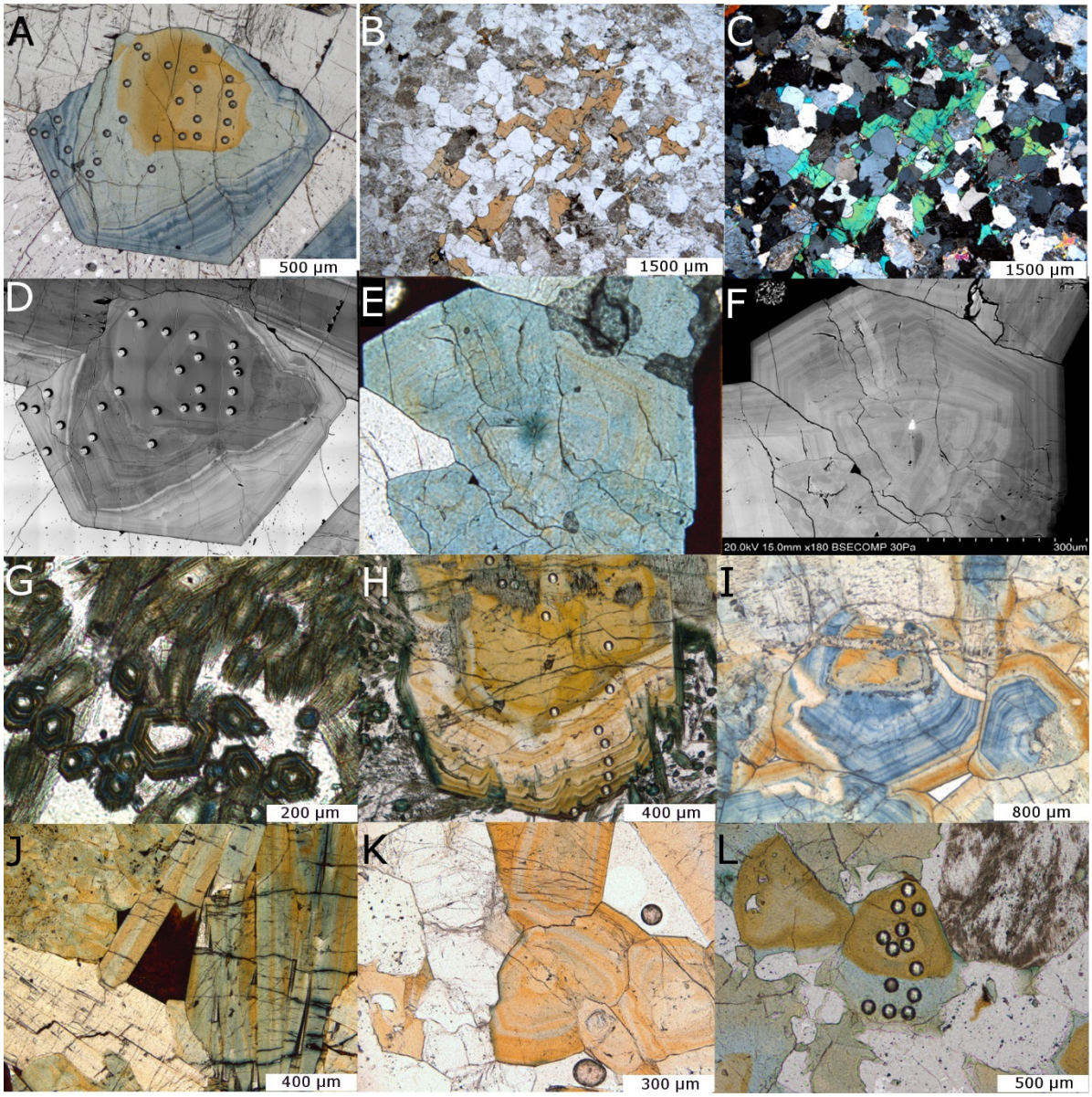

Figure 2. Overview of tourmaline types. All pictures are acquired under plane polarised light except C (cross-polarised), and D and F (backscatter electron). Circular pits are holes from LA-ICP-MS analyses. A: Type 1 (brown), type 2 (weakly oscillatory zoned light blue to light brown, and type 3 (oscillatory zoned dark to light blue) tourmaline from sample KDC-17-03. B: Interstitial type 1 tourmaline from the matrix of a tourmaline granite (sample KDC-16-13). C: Same as B in cross-polarised light showing optical continuity. D: BSE image of A showing minor resorption of type 1 by type 2 and variations in mean atomic number between type 2 and 3. The bright phase surrounding tourmaline is apatite. E: Type 2 tourmaline from the tourmaline zone of sample KDC-16-19-a. F: BSE image of E showing the fine oscillatory zoning pattern not easily observed in the optical microscope. G: Type 5 tourmaline from sample KDC-16-18. Strongly zoned with a colourless core and green and blue rims. This type is typically greenish in sections not normal to the c-axis. H: Type 1 (brown), type 5 (green), type 6 (pale blue-green overgrowth in the upper and right part of the picture), and type 7 (oscillatory zoned colourless-brown rim of the large grain) from sample KDC-16-18. I: Type 1, 2, 3, and 6 from sample KDC-17-02. J: Type 4 tourmaline from sample KDC-16-05. K: Type 2 tourmaline from sample KDC-16-08. L: Type 1 and 2 from sample KDC-17-12.

Type 4 tourmaline is strongly zoned from greenish blue to brown. The zoning is either oscillatory or patchy. Sections normal to the c-axis have a green-blue core and a brown rim. Type 4 tourmaline replace K-feldspar in the granite bordering various quartz-tourmaline structures, and is the main constituent in addition to quartz in a coarse grained quartz-tourmaline sheet (Fig. 2j).
Type 5 tourmaline is strongly oscillatory zoned with a colourless core and a dark blue rim. However, the major growth zones are green, and sections parallel to the c-axis are characteristically pleochroic from colourless to green with an acicular crystal shape. Type 5 tourmaline is ubiquitous in veins and hydrothermal replacement textures (Figs. 2 g and 2h). It is also common in some larger quartz-tourmaline bodies.
Type 6 tourmaline typically occurs as pleochroic colourless to blue overgrowth of other generations of tourmaline. In granite and all quartz-tourmaline aggregations, type 6 tourmaline also occurs as inclusions, likely replacing former feldspar inclusions (Fig. 2h). A stage of brown tourmaline overgrowing all other generations is also included in this type. This is only observed in one sample of miarolitic tourmaline (Fig. 2i).
Type 7 tourmaline covers strongly oscillatory zoned, pleochroic, colourless to brown tourmaline overgrowing type 1. This type was found in replacement textures and a large quartz-tourmaline body (Fig. 2h).

3.3. Mineral chemistry

Tourmaline is divided into primary groups and general series based on their X-site and W-site occupancy, respectively [15]. Most analyses plot (Fig. 3) in the alkali group, with a few type 3 points in the vacancy group, and a few type 5 and 6 in the calcic group. There is a larger spread between the types in the W-site diagram, where types 1, 2 and most of type 3 tourmaline are fluorine-species, and types 5 and 7 are hydroxyl-species. Types 4 and 6 are divided between the fluorine- and hydroxyl-groups. Two smaller clusters of type 3 tourmaline plot in the oxy-field and on the border between oxy- and hydroxyl-groups. A similar grouping is observed in the Fe/Fe+Mg versus X-vacancy plot. Types 1 - 4 are generally schorl, a few points plotting in the foitite field, and types 5 - 7 are generally dravite. From this we can distinguish two main groups of tourmaline in the Land's End granite: F-schorl and dravite. Tourmaline classifying as F-dravite is late brown overgrowths (included in type 6) in sample KDC-17-03 and strongly oscillatory zoned tourmaline (type 7) in sample KDC-16-18.

Substitution of Fe for Mg is the main controlling substitution in tourmaline in granitic systems. The strong chemical zoning in type 5 and 7 tourmaline is largely due to variation in the Fe and Mg content, hence the large spread of these types in the Fe/(Fe+Mg) versus X-vacancy plot. The gradual or stepwise growth zoning shown in tourmaline of type 1 - 3 combined with the gradual increase in Fe may indicate differentiation in a closed system, from a dominantly magmatic (type 1) to a more aqueous fluid-dominated system (type 3). The dravitic types 5 - 7 tourmalines represent a different crystallisation mode. Texturally, these tourmaline types are clearly hydrothermal in origin, and the fluid was more evolved compared to type 3 tourmaline, or possibly mixed with other fluid sources. The latter hypothesis is also evident in the Sn versus Sr plot, where type 1 - 3 show increasing levels of both Sn and Sr, two elements likely to partition into saline aqueous fluids. Types 5 - 7 are the richest in Sr and Sn, giving them a strong hydrothermal signature. Particularly, type 5 is known to be associated with cassiterite mineralisation [11]. The different types showed great separation in the Ni-Co-Zn diagram. Fe and Ti have been proposed to be the main chromophores in tourmaline [16]. However, the clear separation in Fig. 3 may indicate that these elements play also a role.

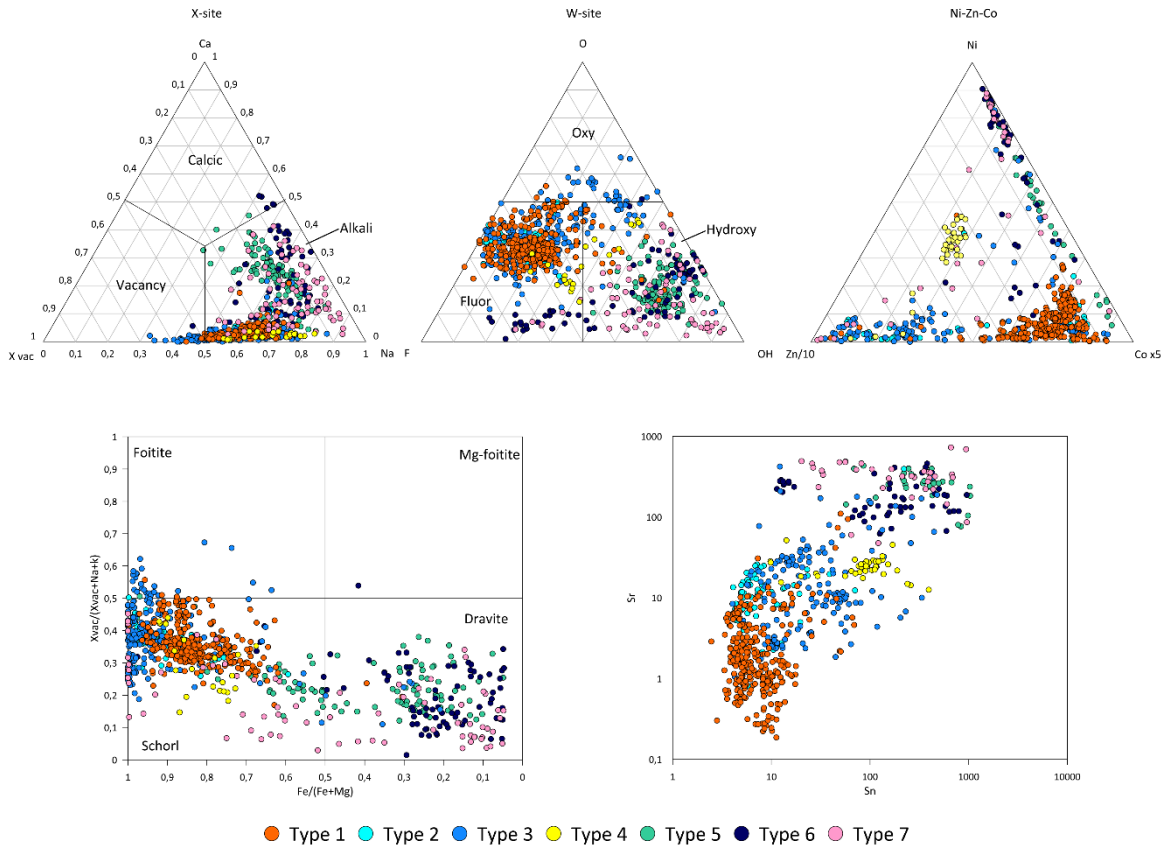

Figure 3. Chemical plots of tourmaline from this study. The colours largely reflect the colour observed in plane polarised light. Most type 2 points are covered by type 1 and 3 points.

4. Conclusions

Seven types of tourmaline were distinguished in samples from the southern part of the Land's End granite. These were primarily discriminated based on colour and growth textures. The different types can also be identified in major and trace element plots. Two main groups, F-schorl and dravite, represent closed magmatic-hydrothermal and open hydrothermal system crystallisation, respectively. A differentiation path can be distinguished within the magmatic-hydrothermal tourmaline from the center of the schorl field towards more Fe-rich composition.

Acknowledgements

We thank Darrell Henry for a constructive review that helped improve the paper.

References

[1] van Hinsberg V J, Henry D J and Marschall H R 2011 Tourmaline: an ideal indicator of its host environment. *Can. Mineralogist* **49** 1-16

[2] Farnsworth-Pinkerton S, McMillan N J, Dutrow B L and Henry D J 2018 Provenance of detrital tourmalines from Proterozoic metasedimentary rocks in the Picuris Mountains, New Mexico, using laser-induced breakdown spectroscopy. *J. Geosci.* **63** 193-198

[3] Henry D J and Guidotti C V 1985 Tourmaline as a petrogenetic indicator mineral- An example from the staurolite-grade metapelites of NW Maine. *Amer. Mineralogist* **70** 1-15

[4] Henry D J and Dutrow B L 1992 Tourmaline in a low grade clastic metasedimentary rock: an example of the petrogenetic potential of tourmaline. *Contr. Mineral. Petrol.* **112** 203-218
[5] Hervig R L, Moore G M, Williams L B, Peacock S M, Holloway J R and Roggensack K 2002 Isotopic and elemental partitioning of boron between hydrous fluid and silicate melt. *Amer. Mineralogist* **87** 769-774
[6] London D, Hervig R and Morgan G V I 1988 Melt-vapor solubilities and elemental partitioning in peraluminous granite-pegmatite systems: experimental results with Macusani glass at 200 MPa. *Contr. Mineral. Petrol.* **99** 360-373
[7] Pichavant M 1981 An experimental study of the effect of boron on a water saturated haplogranite at 1 Kbar vapour pressure. *Contr. Mineral. Petrol.* **76** 430-439
[8] Slack J F 1996 Tourmaline associations with hydrothermal ore deposits. *Rev. Mineral. Geochem.* **33** 559-643
[9] Taylor J R and Wall V J 1993 Cassiterite solubility, tin speciation, and transport in a magmatic aqueous phase. *Econ. Geol.* **88** 437-460
[10] Yavuz F, Yavuz V and Sasmaz A 2006 WinClastour—a Visual Basic program for tourmaline formula calculation and classification. *Comp. Geosci.* **32** 1156-1168
[11] Drivenes K, Larsen R, Müller A, Sørensen B, Wiedenbeck M and Raanes M 2015 Late-magmatic immiscibility during batholith formation: assessment of B isotopes and trace elements in tourmaline from the Land's End granite, SW England. *Contr. Mineral. Petrol.* **169** 1-27
[12] Rozendaal A and Bruwer L 1995 Tourmaline nodules: indicators of hydrothermal alteration and Sn-Zn-(W) mineralization in the Cape Granite Suite, South Africa. *J. African Earth Sci.* **21** 141-155
[13] Perugini D and Poli G 2007 Tourmaline nodules from Capo Bianco aplite (Elba Island, Italy): an example of diffusion limited aggregation growth in a magmatic system. *Contr. Mineral. Petrol.* **153** 493-508
[14] Drivenes K, Larsen R B, Müller A and Sørensen B E 2016 Crystallization and uplift path of late Variscan granites evidenced by quartz chemistry and fluid inclusions: Example from the Land's End granite, SW England. *Lithos* **252–253** 57-75
[15] Henry D J, Novák M, Hawthorne F C, Ertl A, Dutrow B L, Uher P and Pezzotta F 2011 Nomenclature of the tourmaline-supergroup minerals. *Amer. Mineralogist* **96** 895-913
[16] London D, Morgan G B and Wolf M 1996 Boron in granitic rocks and their contact aureoles. in: *Boron : mineralogy, petrology and geochemistry*. *Rev.Mineral.* **33** 299-330